Electronic structure studies of V_6O_{13} by soft x-ray emission spectroscopy: Band-like and excitonic vanadium states

T. Schmitt,[1,*] L.-C. Duda,[1] M. Matsubara,[2,†] M. Mattesini,[1] M. Klemm,[3] A. Augustsson,[1] J.-H. Guo,[4] T. Uozumi,[5] S. Horn,[3] R. Ahuja,[1] A. Kotani,[2,‡] and J. Nordgren[1]

[1]*Department of Physics, Uppsala University, Ångström Laboratory, Box 530, S-75121 Uppsala, Sweden*

[2]*Institute for Solid State Physics, The University of Tokyo, 5-1-5 Kashiwanoha, Kashiwashi, Chiba 277-8581, Japan*

[3]*Experimentalphysik II, Institut für Physik, Universität Augsburg, D-86135 Augsburg, Germany*

[4]*Advanced Light Source, Lawrence Berkeley National Laboratory, MS 7-222, One Cyclotron Road, Berkeley, California 94720, USA*

[5]*College of Engineering, Osaka Prefecture University, Sakai, Osaka 599-8531, Japan*

(Received 12 November 2003; published 12 March 2004)

Resonant soft x-ray emission (SXE) spectra of the mixed valence vanadium oxide V_6O_{13} have been recorded for a series of excitation energies across the V L-absorption band. Resonant excitation allows one to distinguish between charge neutral low-energy excitations and continuum-excited, more band-like V $3d$ valence band states in the spectra. We find that the V L-emission spectra of V_6O_{13} consist of two distinct components that can be assigned to nearly pure V $3d$ states, and to V $3d$ states that are strongly hybridized with O $2p$ states, respectively. Band structure calculations of the density functional theory support the assignment of these features. At threshold excitation the V L-emission spectra of V_6O_{13} show strong signatures from excitonic states, the energy dependence of which shows Raman-like behavior. We compare these spectral features in the resonant SXE spectra with cluster model calculations and assign them to dd excitations and charge-transfer excitations, respectively. Finally, we discuss changes in the V L-absorption and emission spectra that take place when changing the sample temperature from 295 K to 120 K. We relate the changes to redistributions in the V $3d$ partial density of states, which occur at the transition temperature for the metal-semiconductor-transition $T_{MST}=150$ K and find support in our temperature dependent band structure calculations.

DOI: 10.1103/PhysRevB.69.125103 PACS number(s): 71.27.+a, 78.70.En, 71.20.−b, 71.30.+h

I. INTRODUCTION

Vanadium oxides comprise a particularly interesting subgroup of the $3d$ transition metal compound family due to the large variety of electronic, magnetic and structural properties, and notably their metal-to-insulator or metal-to-semiconductor transitions[1] (MST). Vanadium oxides also possess interesting technological aspects, for instance in catalytic applications and they receive strong attention as model systems for novel compact rechargeable lithium batteries where Li is inserted into the cathode material. V_6O_{13}, for example, is being used as an active electrochemical component in cathodes of lithium batteries.[2]

V_6O_{13} is a monoclinic mixed valence compound (electron configuration: $4\,V^{4+}+2\,V^{5+}$) that undergoes a MST at 150 K that is accompanied by a structural distortion from the paramagnetic metal phase with $C2/m$ symmetry[3,4] to the paramagnetic semiconducting phase with $C2$ symmetry[4] or $P2_1/a$ symmetry.[5] Antiferromagnetic order occurs below ca. 55 K.[6] The basic building blocks of the crystal are distorted VO_6 octahedra[3,4] which form two types of sheets parallel to the a-b plane. One zigzag VO_6 chain running along the b axis is monovalent (V^{4+}) and a second chain is of mixed valency (alternating V^{4+} and V^{5+}).[3,4] Electrical resistivity measurements[7] and an optical reflection study[8] revealed a highly anisotropic behavior suggesting a quasi-one-dimensional electronic structure which was corroborated by a recent angle-resolved photoemission study.[9] As some of the few studies of the electronic structure of V_6O_{13}, ordinary photoemission spectroscopy[10] (PES) and angular resolved photoemission spectroscopy[9] (ARPES) have been used to study the valence bands of V_6O_{13}. With x-ray absorption spectroscopy[11] one has studied the empty vanadium $3d$ and oxygen $2p$ states. Particular attention has been paid to the MST of V_6O_{13}. Small changes in the valence band width have been observed by PES, however, the trends of ordinary PES and ARPES appear to be of opposite nature, i.e., band narrowing is observed upon cooling in ordinary PES and band broadening in ARPES. Both experiments, however, seem to show a systematic gap opening at the Fermi level, as would be expected for the transition to the semiconducting state. Calculations of the electronic band structure of V_6O_{13} have, to our knowledge, not been reported so far.

In this paper, we investigate the electronic structure of V_6O_{13} single crystals by means of soft x-ray absorption (SXA) spectroscopy and resonant soft x-ray emission (SXE) spectroscopy. By measuring the SXA spectrum we can determine specific excitation energies for our resonant SXE experiments. We present a combined experimental and theoretical analysis of the electronic structure of V_6O_{13} focusing on the role and interplay of bandlike and localized excitations close to the ground state. We also use SXA and SXE spectroscopy at the V L edges to monitor changes in the electronic structure across the MST of V_6O_{13}.

SXE is a two-photon scattering process and the spectra accurately reflect the local partial density of states (LPDOS) for less correlated materials. In SXE spectroscopy a core electron is excited by an x-ray photon, promoting the atom to an intermediate core-excited (but neutral) state. This intermediate state can decay radiatively to a valence-excited state or

to the ground state. The energy difference of the incoming and outgoing photons is taken up by the electronic system. Often there are quantized excitations (crystal field excitations) that become resonantly enhanced at certain excitation energies and therefore we call this type of spectrum resonant inelastic x-ray scattering (RIXS).[12] These low energy local electronic excitations (e.g., dd excitations) disperse linearly with the incoming photon energy, as in optical Raman scattering. The part of the resonant SXE spectra that does not behave as Raman scattering, and thus is stationary in x-ray emission energy, is referred to as ''ordinary fluorescence.'' [13] This ordinary fluorescence part originates from continuum excited intermediate states and can be related to the LPDOS of the material. Thus resonant SXE spectra generally consist of three ''subcomponents:'' (1) ordinary fluorescence at fixed x-ray emission energy, (2) RIXS contributions at constant energy loss, and (3) elastic scattering at the incoming photon energy. Local electronic excitations are often significant in correlated $3d$-transition metal compounds, such as vanadates, and give prominent RIXS contributions in L-edge SXE spectra. In conventional optical absorption techniques transitions between states with the same angular momentum quantum number l are dipole forbidden and very weak, and therefore often obscured by other spectral features. The study of charge-neutral low-energy local excitations by RIXS is therefore superior to optical absorption investigations.

II. EXPERIMENT

V_6O_{13} single crystals were grown in a gradient furnace by chemical transport reaction, using $TeCl_4$ as a transport agent at a growth temperature of 630 °C. X-ray powder diffraction on powdered single crystals revealed no spurious phases and Laue diffraction showed the crystals to be of high quality. The electrical resistivity measured as a function of temperature revealed the expected MST at $T=150$ K. The investigated V_6O_{13} sample was a single crystal with dimensions of approximately $2\,\text{mm}\times 2\,\text{mm}\times 0.1\,\text{mm}$. Experiments were performed at room temperature and at 120 ± 2 K when cooling the sample holder with liquid nitrogen.

SXA and SXE experiments were performed at the undulator beam lines 7.0.1 (Ref. 14) at the Advanced Light Source (Lawrence Berkeley National Laboratory, USA) and I511-3 (Ref. 15) at MAX II (MAX-lab National Laboratory, Lund University, Sweden). Beamline I511 comprises a modified SX-700 monochromator layout and beamline 7.0.1 is based on a spherical grating monochromator design. SXA spectra were measured by recording the total electron yield (TEY) by measuring sample drain current while scanning the photon energy of the incident monochromatized synchrotron radiation. The SXA spectra were normalized to the photocurrent from a gold mesh introduced into the synchrotron radiation beam in order to correct for intensity variations of the incident x-ray beam. SXE was recorded with a high-resolution Rowland-mount grazing-incidence grating spectrometer[16] with a two-dimensional detector using a spherical grating of 5 meter radius with 1200 lines/mm in first order of diffraction giving a spectrometer energy resolution of better than 0.4 eV for energies around 515 eV. The monochromator spectral bandwidth chosen for the SXA spectra and for the excitation of the resonant SXE spectra was set to 0.15 eV and 0.3 eV, respectively. The total energy resolution (combined from excitation and spectrometer energy resolution) of the SXE experiments was approximated to be 0.6 eV by measuring the FWHM (full width at half maximum) at the elastic peaks. The x-ray emission energy was calibrated by recording the characteristic Zn $L_{\alpha,\beta}$ spin-orbit doublet in 2nd order of diffraction, i.e., the $3d$-$2p_{3/2,1/2}$ transitions, from a pure Zn foil and using the tabulated characteristic x-ray line energies from Ref. 17. A common energy scale for SXE and SXA spectra was determined from the peak positions of the elastically scattered x-rays in the resonant SXE spectra.

III. THEORY: BAND STRUCTURE CALCULATIONS AND CLUSTER MODEL CALCULATIONS

V L x-ray emission spectra have been calculated within the local density approximation of the density functional theory using the augmented plane wave and local orbital (APW+lo) band structure method.[18] Exchange and correlation effects were treated within the density functional theory (DFT)[19] by using the generalized gradient approximation (GGA).[20] It should be noted that we have not included any many-body effects such as the influence of the core hole on the band states and interactions between the excited electron and the core hole. For the transition matrix elements the electric-dipole approximation has been employed, i.e., only transitions between the core state with orbital angular momentum l to the $l\pm 1$ components of the conduction band have been considered. The next Sec. IV A compares the V L-emission spectrum gained from the band structure calculations to the ordinary fluorescence part of the V L-SXE spectra.

The experimental V L-RIXS spectra presented in Sec. IV B are compared to model calculations. These calculations were performed in octahedral (O_h) symmetry with a single vanadium site VO_6 cluster model[21] in the framework of an Anderson impurity model.[12] For V_6O_{13} the basic structural units consist of distorted VO_6 octahedra connected in the a-b plane to layers.[3,4] The distorted VO_6 octahedra are represented in the calculations by the single vanadium site VO_6 clusters. V_6O_{13} is in a mixed valence state with a formal valency of ''$4\,V^{4+}+2\,V^{5+}$.'' [3,4,6] In order to account for this mixed valency, spectra were calculated using the Kramers-Heisenberg formula[12,21] for the V^{4+} and V^{5+} oxidation states of the mixed valence chain and for V^{4+} of the monovalent chain, respectively. The independently calculated spectra are then superimposed.

The adjustable parameters of the Anderson impurity Hamiltonian for the V L-RIXS model calculations for vanadium oxides are the charge transfer energy $\Delta = E(d^{n+1}\underline{L})$-$E(d^n)$ between V $3d$ and ligand O $2p$ orbitals, the on-site d-d Coulomb interaction U_{dd}, the intra-atomic core hole potential U_{dc}, the hybridization strength $V(e_g)=-2V(t_{2g})$ and the magnitude of the crystal field splitting $10\text{Dq}=\varepsilon(e_g)$-$\varepsilon(t_{2g})$. Further details about the theoretical calculations and the formulation of the chosen cluster model

TABLE I. Adjustable parameters of the cluster model Hamiltonian for V_6O_{13}.

		Δ	U_{dd}	U_{dc}	$V(e_g)$	10 Dq
Mixed valent chain	V^{4+}	4.0 eV	4.0 eV	4.8 eV	3.1 eV	0.7 eV
	V^{5+}	0 eV	4.0 eV	4.8 eV	3.1 eV	0.7 eV
Monovalent chain	V^{4+}	2.5 eV	5.0 eV	6.0 eV	3.0 eV	0.7 eV

Hamiltonian are described elsewhere.[21] Table I lists the used parameter values of the calculated RIXS spectra for V_6O_{13}. A direct comparison between the experimental and calculated V L-RIXS spectra is presented in Sec. IV B.

IV. RESULTS

A. Ordinary fluorescence of V_6O_{13}: Bandlike states

In Fig. 1 we show the V L and O K SXA-TEY spectrum of V_6O_{13} which is very similar to that obtained in Ref. 11. Also shown is the V L-SXA spectrum of our multiplet cluster model calculation (bottom curve). Between 513 eV and 528 eV the V L-spectrum is split into the spin-orbit doublet. The absorption band from 513 to 521 eV is derived from the V $2p_{3/2} \rightarrow$ V $3d$ transition (V L_3) and the one from 521 to 528 eV from the V $2p_{1/2} \rightarrow$ V $3d$ transition (V L_2). Just above the V L_2 edge (528 eV) Fig. 1 displays the part of the O K SXA spectrum that originates from O $2p$ states hybridized with crystal field split V $3d$ states (t_{2g} and e_g).

Figure 2 shows the resonant SXE spectra of V_6O_{13} excited at the energies indicated by the arrows A–I in the SXA spectrum in Fig. 1. We observe the evolution of the V L_α band ($3d \rightarrow 2p_{3/2}$) and the V L_β band ($3d \rightarrow 2p_{1/2}$), situated around 510 eV and 518 eV, respectively, as we tune the excitation energy across the L edges. The overlap of the V L_α and V L_β band is caused by the relatively small spin-orbit splitting between the $2p_{1/2}$- and $2p_{3/2}$-core states and we marked the approximate extent of the bands with the black

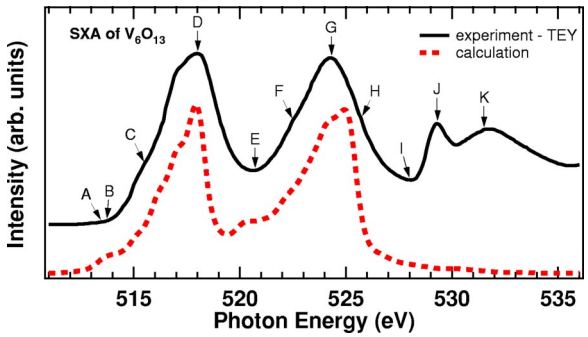

FIG. 1. (Color online) V L and O K soft x-ray absorption spectra of V_6O_{13} in total electron yield mode (top curve) compared to the multiplet cluster model calculation of the V L absorption spectrum (bottom curve). The excitation energies for the resonant soft x-ray emission spectra in Fig. 2 are marked by arrows above the spectrum.

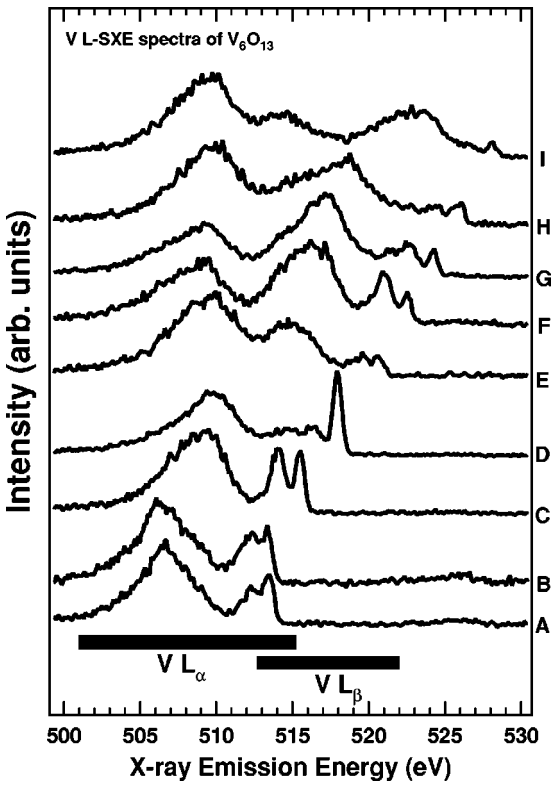

FIG. 2. Resonant soft x-ray emission spectra of V_6O_{13} excited at the energies indicated by the arrows A–I in the absorption spectrum in Fig. 1. The energy regions of the overlapping V L_α- and V L_β-emission bands are marked through bars at the energy scale.

bars at the bottom of Fig. 2. By tuning the energy below the $2p_{1/2}$-absorption threshold only the V L_α band appears in the SXE spectrum leaving it unobscured by the V L_β band (spectra A–D). Note that one can observe in spectrum D how excitonic parts, the elastic peak at 518 eV and a dd-excitation peak at 516.4 eV (explained in more detail in the next section), of the spectrum start to separate from the continuum-excited part (below 516 eV). Similar effects as for the V L_α band are observed for the V L_β band at higher excitation energies, although including distortions by the mentioned overlap.

Figure 3 shows a comparison between the experimental V L_α-SXE spectrum excited at the maximum of the V L_3 absorption band at energy D (second curve from the bottom) and the spectrum derived from our LDA band structure calculation (third spectrum from the bottom). The degree of agreement indicates to what extent the V L_α-SXE spectra reflect the V $3d$ and O $2p$ PDOS, respectively. The calculations show, first, that there is one high-energy narrow band, derived from states having almost purely V $3d$ character and secondly, that there is a broad band of states at lower energies that derive from O $2p$ states and are strongly hybridized with V $3d$ states. The energy positions of both bands are marked at the energy scale of Fig. 3. We aligned all spectra in Fig. 3 on an energy scale relative to the Fermi level (0 eV) by letting the gap between the two peaks coincide. The energy separations between the two peaks found by the APW

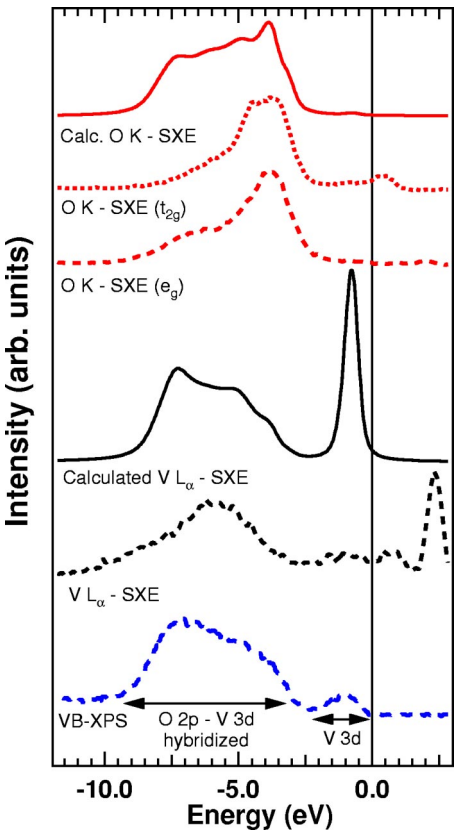

FIG. 3. (Color online) Comparison between experimental V L-(excitation energy D) and O K-emission spectra (excitation energies J and K), and emission spectra derived from band structure calculations within the APW+lo approach. A valence band XPS spectrum (Ref. 21) is also shown. The energy position of the two main spectral contributions, pure V $3d$ states and O $2p$–V $3d$ hybridized states, are indicated at the energy scale.

+lo PDOS calculation and the SXE experiment are in good agreement. For comparison we also show valence band x-ray photoelectron spectroscopy (VB-XPS) data taken by Demeter *et al.*[22] (bottom curve); see also Refs. 9, 10, and 23. Judging by the shape of the low-energy peak we conclude that the VB-XPS mainly reflects the states at the V sites. The deviations of the V L_3-excited SXE spectrum from the one derived from the PDOS is probably a consequence of correlation and multiplet splitting effects.

Turning our attention to the oxygen $2p$-PDOS and the O K-SXE spectra in Fig. 3 (top three spectra), we note that they also show the two basic spectral features at a similar energy separation. However, the intensity of the high energy peak is very small in this case and the spectral weights in the low energy peak are different from those of the spectrum derived from the V $3d$ PDOS. This behavior is similar in the two resonantly excited oxygen spectra shown in Fig. 3. Note that variations in spectral shape between the two oxygen spectra are a consequence of exciting at two different energies. These energies are assumed to correspond to t_{2g} and e_g oxygen states (excitation energies J and K in Fig. 1), respectively, whereby the effect of shifts from inequivalent oxygen sites probably plays a minor role.

B. RIXS of V_6O_{13}: dd and charge transfer excitations

A prominent feature in the resonantly excited SXE spectra A–I of Fig. 2 at the V L thresholds disperses linearly with the elastic peak at an energy loss of approximately -1.6 eV. We assign this loss structure to a local dd excitation within the crystal field split $3d$ multiplet ($e_g \rightarrow t_{2g}$). This is in good agreement with optical reflectivity data and the derived absorption spectra that show structures in the range 0.5–1.8 eV.[8] The authors of Ref. 8 ascribed these structures to transitions within the V $3d$ band system which we refer to as dd excitations in a more localized way of viewing. We point out that RIXS investigations on the related system NaV_2O_5 revealed a dd excitation with very similar loss energy.[13,24] There is some confusion about the origin of this excitation seen in NaV_2O_5 in the literature[24] where this peak has been interpreted as a transition across the correlation gap[25] of NaV_2O_5. V_6O_{13} is a mixed valence compound with both V^{4+} and V^{5+} sites, whereas NaV_2O_5 has equivalent sites with a fractional oxidation state of $V^{4.5+}$. The similarity between the resonance behavior and energy positions of this peak in (metallic) V_6O_{13} and in (insulating) NaV_2O_5 strongly suggests that it has the same origin in both compounds, namely a local dd excitation.

In Fig. 2 we also observe a low-energy band around 507 eV emission energy in the first spectrum A. In Fig. 4 we replotted our resonant SXE spectra A–I against an energy loss scale relative to the elastic peaks, in order to facilitate an easier identification of excitonic features. The same part of the spectra A–C is also seen in Fig. 4 as a band situated around an energy loss of -7 eV. This feature shows more complicated excitation energy dependence than the local dd excitation. Our cluster model calculation (Fig. 5) shows that charge transfer (CT) states ($V3d^2\,\underline{L}$ and $V3d^1\,\underline{L}$) are expected to show up at similar energy losses. Obviously our cluster model calculations give a good account for the dd-excitation peak that is marked by dashed lines at a constant energy loss of -1.6 eV in the experimental spectra (Fig. 4). The spectral overlap in spectra E–I, however, makes it difficult to compare the spectral shapes of the theoretical CT band with the experimental spectra. Nevertheless, even for the unobscured spectra A–E there is less good agreement between this peak and the cluster model calculations than for the low-energy dd peak.

Continuum-excited ordinary fluorescence contributions become increasingly significant for higher excitation energies. Spectra A–C in Fig. 4 mainly consist of RIXS contributions. Beginning with spectrum D, which is excited at the maximum of the V L_3 absorption band, the CT band overlaps with the continuum excited V L_α emission. In the same spectrum, a peak at lower energy appears, adjacent to the dd-excitation peak, and is ascribed to nearly pure V $3d$ states of the V $3d$ PDOS. Spectra D–I show a superposition of coherent RIXS and incoherent ordinary fluorescence contributions leading to deviations between model and experiment. Note that ordinary fluorescence follows from an incoherent process and is therefore not reflected in our cluster model RIXS calculations. The presented band structure calculations (Sec. IV A), on the other hand, are more suitable to

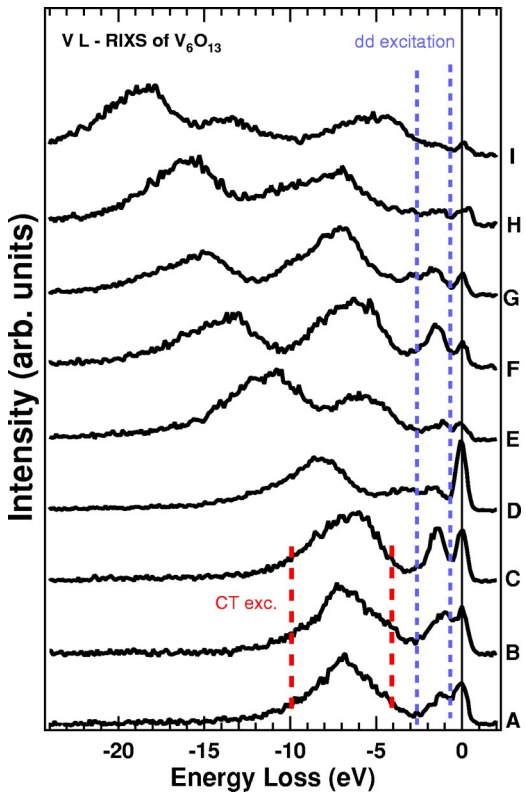

FIG. 4. (Color online) Experimental resonant inelastic x-ray scattering spectra of V_6O_{13} excited at V L-edge energies indicated by the arrows A–I in the absorption spectrum in Fig. 1. The spectra are plotted against an energy loss scale relative to the elastic peaks in the resonant soft x-ray emission spectra of Fig. 2. A peak at an energy loss of approximately -1.6 eV corresponding to a dd excitation and a band of charge transfer states around -7 eV are marked through dashed lines.

compare with the continuum excited ordinary fluorescence part of the resonant SXE spectra (see Fig. 3).

The occurrence of substantial excitonic RIXS contributions in the V L SXE spectra is an indication for the partly correlated nature of the electronic structure of V_6O_{13}. Furthermore, the ratio of coherent to incoherent contributions gives a measure of the localization in the intermediate core-hole state. The intensity of the dd excitation resonates in spectrum C and in spectrum F which were excited at the low-energy shoulders of the corresponding V L-absorption peaks, suggesting that the intermediate states in this energy region are strongly localized.

C. Metal-semiconductor transition in V_6O_{13}

The top panel of Fig. 6 displays two SXA spectra of V_6O_{13}, one recorded at room temperature (RT) and the other one recorded at 120 K, well below the MST temperature of 150 K. In going from the metallic RT phase to the semiconducting phase at 120 K we observe that the VL_3 and VL_2 absorption spectra experience a rigid energy shift and thus the thresholds appear at about 0.1 eV lower photon energies. In Ref. 9 and Ref. 10 a similar shift of 0.15–0.2 eV was reported in valence band photoemission studies of the occupied V3d PDOS.

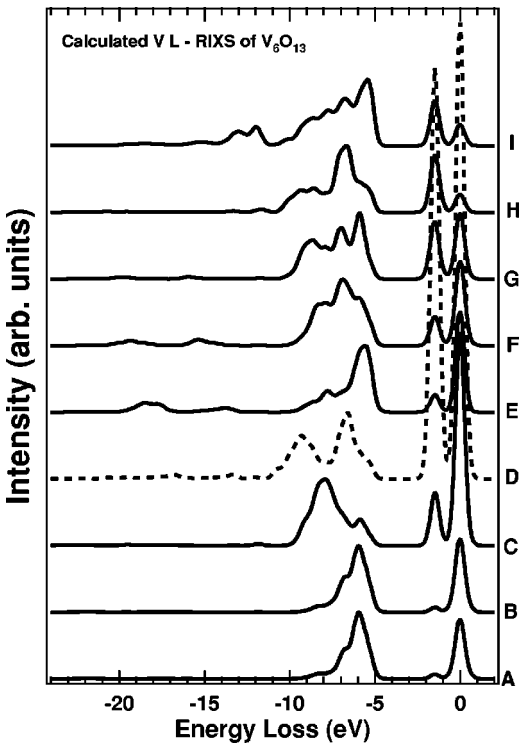

FIG. 5. Calculated RIXS spectra at the V L edges. The spectra are calculated with a single vanadium site VO_6-cluster model for the excitation energies of the experimental RIXS spectra in Fig. 4.

V L_α-SXE spectra excited with synchrotron radiation corresponding to the maximum of the VL_3 absorption band are compared in Fig. 6 (bottom panel) for the metallic (RT) and semiconducting phases (120 K) of V_6O_{13}. As explained in Sec. IV A, such an excitation predominantly projects out the occupied V3d PDOS. Both SXE spectra in Fig. 6 are normalized to the integrated intensity of the O $2p-$V $3d$ hybridized part of the spectra. Clearly, the pure V $3d$ band loses relative spectral weight when the system is cooled to 120 K. Also the center of gravity of the V $3d$ PDOS is shifted about 0.2 eV to higher x-ray emission energies in the semiconducting phase and the spectral width of the pure V $3d$ PDOS is reduced by some 0.2–0.3 eV. This reduced bandwidth might be explainable with increased charge localization on V sites in the semiconducting phase.[6,9,10] The spectral weight of the dd excitation, which can be seen as a faint shoulder at the high energy side of the pure V $3d$ band around 516.8 eV, seems to be unchanged by the MST.

Figure 7 displays calculated V L_3 SXA (top panel) and V L_α-SXE (bottom panel) spectra for $T=100$ K and $T=298$ K. The spectra are derived from band structure calculations of the MST and are displayed for the three inequivalent vanadium sites and for the sum of these sites. These theoretical spectra show the same trend as the corresponding experimental spectra in Fig. 6. The calculated V L_α-SXE spectra of the semiconducting phase at 100 K are rigidly shifted 0.12 eV to higher energies relative to the calculated spectrum of the metallic RT phase at 298 K. Similarly, the band structure calculations reveal a shift of 0.12 eV to lower energies for the V L_3-SXA spectrum, when assuming a cool-

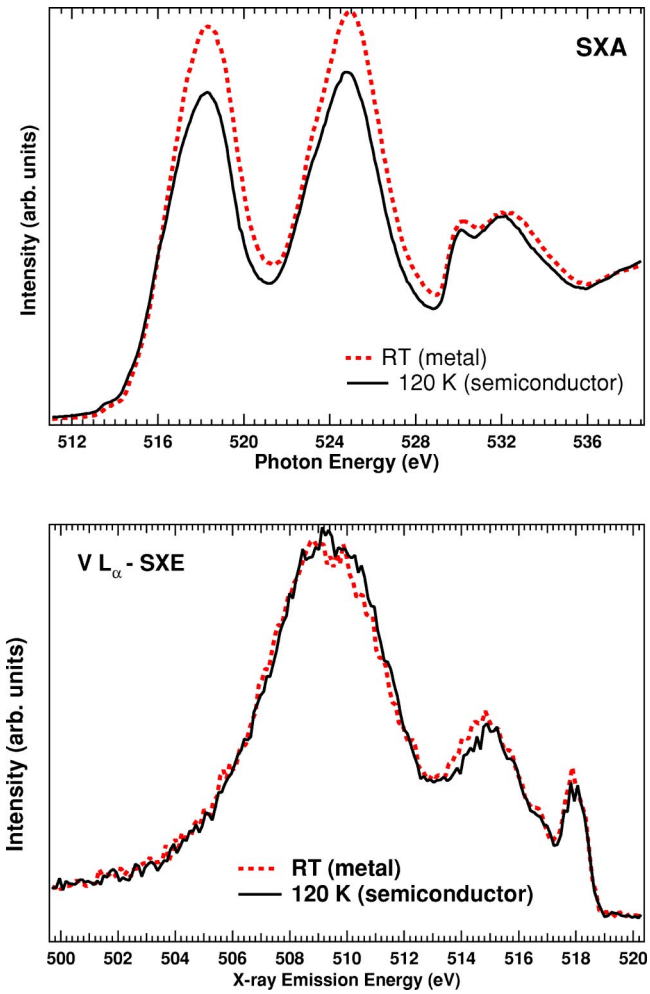

FIG. 6. (Color online) Comparison of V L- and O K-SXA spectra (top panel), and V L_α-SXE spectra (bottom panel) of V_6O_{13} in the metallic phase at room temperature and in the semiconducting phase at 120 K.

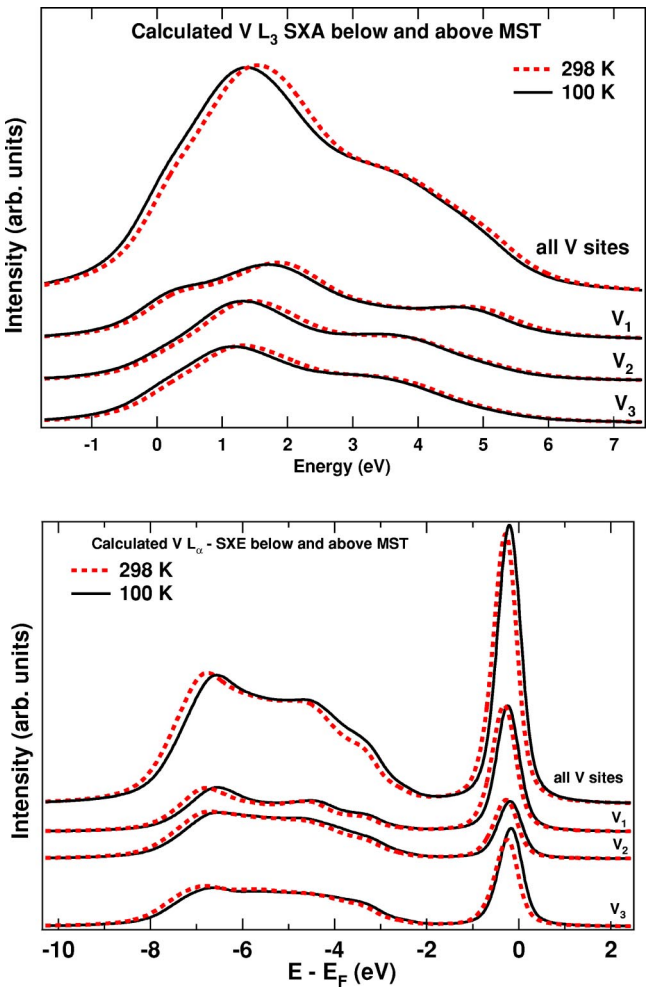

FIG. 7. (Color online) Calculated V L_3 SXA spectra (top panel) and V L_α-SXE spectra (bottom panel) in the metallic phase at 298 K and in the semiconducting phase at 100 K. Spectra are displayed for the three different inequivalent vanadium sites and for the sum of the three sites.

ing of V_6O_{13} from 298 K to 100 K. Nevertheless, the band structure calculations reveal no changes in the bandwidth of the unoccupied V 3d PDOS, which were found in the V L_α-SXE experiment (see above) and previous PES (Ref. 10) and ARPES (Ref. 9) investigations. However, the qualitative agreement between theory and experiment demonstrates that the changes in the electronic structure across the MST are consistent with effects that arise from the small displacements that take place in the crystal structure.

V. DISCUSSION AND CONCLUSIONS

We present a combined theoretical and experimental study of the electronic structure of V_6O_{13}. SXA and resonant SXE spectra were recorded at the V L edges and the O K edge. Resonant excitation allows us to distinguish between charge neutral low-energy excitations and continuum-excited, more band-like V 3d valence band states in the resonant SXE spectra.

The occurrence of both localized excitations and bandlike features in the resonant SXE spectra emphasize the dual nature of the electronic structure of V_6O_{13}. The two theoretical approaches that we present give a good account of each of the specific contributions to the electronic structure. The local low-energy excitations can be simulated by a cluster model calculation using distinct parameters for each of the chains in the crystal. Remarkably, the resonance behavior of the dd excitation differs somewhat in experiment and theory, i.e., we find experimentally that resonance occurs in spectrum C of Fig. 4, whereas theoretically we find the resonance in spectrum D of Fig. 5. A possible reason may lie in coupling between the chains, thus modifying the intermediate core-excited states, which have been neglected in the model calculation. Theory also predicts a rich structure of the charge transfer excitations (Fig. 5), but experimentally this is washed out. Probably, this is due to broadening effects in the real crystal that are absent in our calculation with the present size of our cluster. More sophisticated modeling of the low-energy excitations would also require the use of multisite clusters[26] which is computationally time consuming.

We clearly observe strong hybridization between V 3d

states and O $2p$ states (Fig. 3) as anticipated earlier[9,10] based on PES experiments. Almost pure vanadium $3d$ states are found close to the top of the valence band whereas oxygen $2p$ states and V $3d$ states strongly mix at 3–8 eV below the Fermi level. Continuum excited ordinary fluorescence reflects the PDOS quite well. The intensity of pure V $3d$ states close to the Fermi level is less pronounced in the V L_α-SXE spectrum than in the spectrum gained from the LDA calculation. On the other hand, this behavior is similar to the VB-XPS spectrum of Fig. 3. There is less fine structure of the hybridized O $2p$–V $3d$ peak of the V L_α emission as compared to theory. However, the center of gravity of both peaks fits quite well with the theory. In summary, we may say that atomic multiplet effects, which are of importance for many transition metal oxide L-emission spectra, appear to be of minor significance here and give only rise to small deviations from a mostly bandlike picture of V_6O_{13}.

In our study of the MST of V_6O_{13}, we observe small changes in the V L_α-SXE spectra that reflect the valence band structure. These trends are corroborated by our band structure calculations. We find that the MST of V_6O_{13} is accompanied by changes in the valence band structure in a similar fashion as observed in PES,[9,10] i.e., a small shift of the main V $3d$ band towards the Fermi energy in the semiconducting phase. Our study shows that SXE can give valuable complementary spectroscopic information on the subject of MST in vanadates and the use of brighter x-ray sources would be favorable for a more extensive investigation of the MST with SXE spectroscopy.

ACKNOWLEDGMENTS

This work was supported by the Swedish Research Council (VR) and the Göran Gustafsson Foundation. The Augsburg group is funded in part by the Sonderforschungsbereich 484 of the Deutsche Forschungsgemeinschaft. The experimental work was performed at the Advanced Light Source (ALS) and at MAX-lab. The ALS is supported by the Office of Basic Energy Sciences, Materials Science Division, of the U.S. Department of Energy under Contract No. DE-AC03-76SF00098. We gratefully acknowledge E. Rotenberg (ALS), L. Gridneva (MAX-lab) and C. Glover (MAX-lab) for excellent support and working conditions at beam line 7.0.1 (ALS) and I511 (MAX-lab).

*Corresponding author. Email address: Thorsten.Schmitt@fysik.uu.se

†Present address: Institut de Physique et Chimie des Materiaux de Strasbourg 23, Rue du Loess, BP43, F-67034 Strasbourg Cedex 02, France.

‡Present address: RIKEN/SPring-8, 1-1-1 Kouto, Mikazuki-cho, Sayo, Hyougo 679-5148, Japan.

[1] M. Imada, A. Fujimori, and Y. Tokura, Rev. Mod. Phys. **70**, 1039 (1998); N. F. Mott, *Metal-Insulator Transitions*, 2nd ed. (Taylor and Francis, London, 1990).

[2] T. Gustafsson, J. O. Thomas, R. Koksbang, and G. C. Farrington, Electrochim. Acta **37**, 1639 (1992); T. Schmitt *et al.* (unpublished).

[3] K.-A. Wilhelmi, K. Waltersson, and L. Kihlborg, Acta Chem. Scand. (1947-1973) **25**, 2675 (1971).

[4] P. D. Dernier, Mater. Res. Bull. **9**, 955 (1974).

[5] N. Kimizuka, M. Nakano-Onoda, and K. Kato, Acta Crystallogr., Sect. B: Struct. Crystallogr. Cryst. Chem. **B34**, 1037 (1978).

[6] A. C. Gossard, F. J. Di Salvo, L. C. Erich, J. P. Remeika, Y. Yasuoka, K. Kosuge, and S. Kachi, Phys. Rev. B **10**, 4178 (1974).

[7] K. Kawashima, Y. Ueda, K. Kosuge, and S. Kachi, J. Cryst. Growth **26**, 321 (1974).

[8] W. Van Hove, P. Clauws, and J. Vennik, Solid State Commun. **33**, 11 (1980).

[9] R. Eguchi, T. Yokoya, T. Kiss, Y. Ueda, and S. Shin, Phys. Rev. B **65**, 205124 (2002).

[10] S. Shin, S. Suga, M. Taniguchi, M. Fujisawa, H. Kanzaki, A. Fujimori, H. Daimon, Y. Ueda, K. Kosuge, and S. Kachi, Phys. Rev. B **41**, 4993 (1990).

[11] E. Goering, O. Müller, M. L. denBoer, and S. Horn, Physica B **194**, 1217 (1994); E. Goering, O. Müller, M. Klemm, J. P. Urbach, H. Petersen, C. Jung, M. L. denBoer, and S. Horn, *ibid.* **208**, 300 (1995).

[12] A. Kotani and S. Shin, Rev. Mod. Phys. **73**, 203 (2001).

[13] T. Schmitt, L.-C. Duda, A. Augustsson, J.-H. Guo, J. Nordgren, J. E. Downes, C. McGuinness, K. E. Smith, G. Dhalenne, A. Revcolevschi, M. Klemm, and S. Horn, Surf. Rev. Lett. **9**, 1369 (2002); T. Schmitt, L.-C. Duda, M. Matsubara, A. Augustsson, F. Trif, J.-H. Guo, L. Gridneva, T. Uozumi, A. Kotani, and J. Nordgren, J. Alloys Comp. **362**, 143 (2004).

[14] T. Warwick, P. Heimann, D. Mossessian, W. McKinney, and H. Padmore, Rev. Sci. Instrum. **66**, 2037 (1995).

[15] R. Denecke *et al.*, J. Electron Spectrosc. Relat. Phenom. **101-103**, 971 (1999).

[16] J. Nordgren, G. Bray, S. Cramm, R. Nyholm, J.-E. Rubensson, and N. Wassdahl, Rev. Sci. Instrum. **60**, 1690 (1989).

[17] J. A. Bearden, Rev. Mod. Phys. **39**, 78 (1967).

[18] P. Blaha, K. Schwarz, G. K. H. Madsen, D. Kvasnicka, and J. Luitz, ''WIEN2K, An Augmented Plane Wave+Local Orbitals Program for Calculating Crystal Properties,'' Karlheinz Schwarz, Techn. Universität Wien, Austria, 2001, ISBN 3-9501031-1-2.

[19] W. Kohn and L. J. Sham, Phys. Rev. **140**, A1133 (1965); P. Hohenberg and W. Kohn, Phys. Rev. **136**, B864 (1964).

[20] J. P. Perdew, K. Burke, and M. Ernzerhof, Phys. Rev. Lett. **77**, 3865 (1996).

[21] M. Matsubara, T. Uozumi, A. Kotani, Y. Harada, and S. Shin, J. Phys. Soc. Jpn. **69**, 1558 (2000); **71**, 347 (2002).

[22] M. Demeter, M. Neumann, and W. Reichelt, Surf. Sci. **454-456**, 41 (2000).

[23] J. Mendialdua, R. Casanova, and Y. Barbaux, J. Electron Spectrosc. Relat. Phenom. **71**, 249 (1995).

[24] G. P. Zhang, T. A. Callcott, G. T. Woods, L. Lin, B. Sales, D. Mandrus, and J. He, Phys. Rev. Lett. **88**, 077401 (2002).

[25] See, e.g., H. Wu and Q.-Q. Zheng, Phys. Rev. B **59**, 15 027 (1999).

[26] T. Ide and A. Kotani, J. Phys. Soc. Jpn. **67**, 3621 (1998); A. Kotani and T. Ide, J. Synchrotron Radiat. **6**, 308 (1999).